MASTER

UCID- 17877

Lawrence Livermore Laboratory

FORMATION AND TRANSPORT OF A BRIGHT ELECTRON BEAM FOR FLASH X-RAY APPLICATIONS

B. Kulke, H. B. McFarlane and R. Kihara

July, 1978

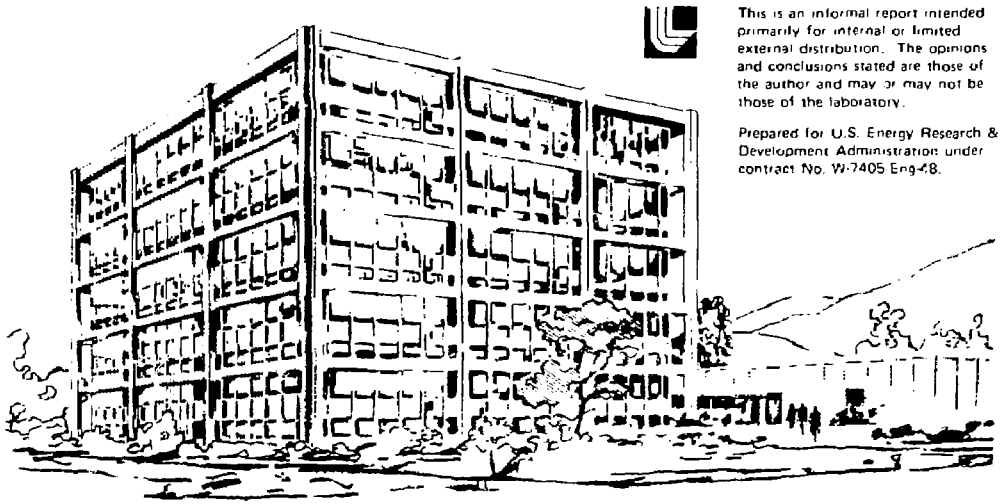

FORMATION AND TRANSPORT OF A BRIGHT ELECTRON BEAM FOR FLASH X-RAY APPLICATIONS

B. Kulke, H. B. McFarlane and R. Kihara

July, 1978

ABSTRACT

Measurements have been carried out to characterize a 1 MeV, 1-5 kA field emitter diode and to determine the emittance of the electron beam generated. The diode was found to be approximately space charge limited, and the beam emittance at 300-500 A of collimated beam was measured at 30 π-70 π mr-cm, depending on the emitter geometry. Simple confinement of the beam over a one metre distance also was demonstrated, using axial magnetic confining fields of less than one kilogauss.

"Work performed under the auspices of the U.S. Department of Energy by the Lawrence Livermore Laboratory under contract number W-7405-ENG-48."

Contents

1. Introduction

The proposed FXR linear induction accelerator (Ref. 1) is expected to deliver a singly pulsed, 16 MeV, 4000 A electron beam to its bremsstrahlung production target. This beam is required to be "bright" in the sense that its nominal spot size of 3 mm or less, translates into an emittance requirement of approximately 0.5 π mr-cm at the target, or 5 π mr-cm at the injector. Present planning favors a field-emitter type of electron source in the injector. In order to gain experience with such a source, an experiment was set up to characterize the beam generated from the five cavity injector section of the LBL/ERA machine (Ref. 2) which had been decommissioned earlier and hence was available. The injector section of this machine was brought to LLL and reactivated, and it has been operating since December 1977. The purpose of this note is to summarize the test results obtained since then.

2. The Injector Test Stand

The LBL/ERA machine had been built as a tandem array of 15 accelerator modules, basically single-turn, ferrite-core pulse transformers, interspersed with thin-lens focusing solenoids. Five of these modules were brought to LLL and reassembled (Fig. 1). They are bolted together to form a single tank, and they are threaded by a metallic stem that carries the emitter electrode. The anode is a planar, wire mesh positioned at an adjustable distance from the cathode. The conducting cathode stem electrically sums the voltage contributions of the five individual accelerating modules, rated at 250 kV each, so that up to 1.25 MV may appear across the diode.

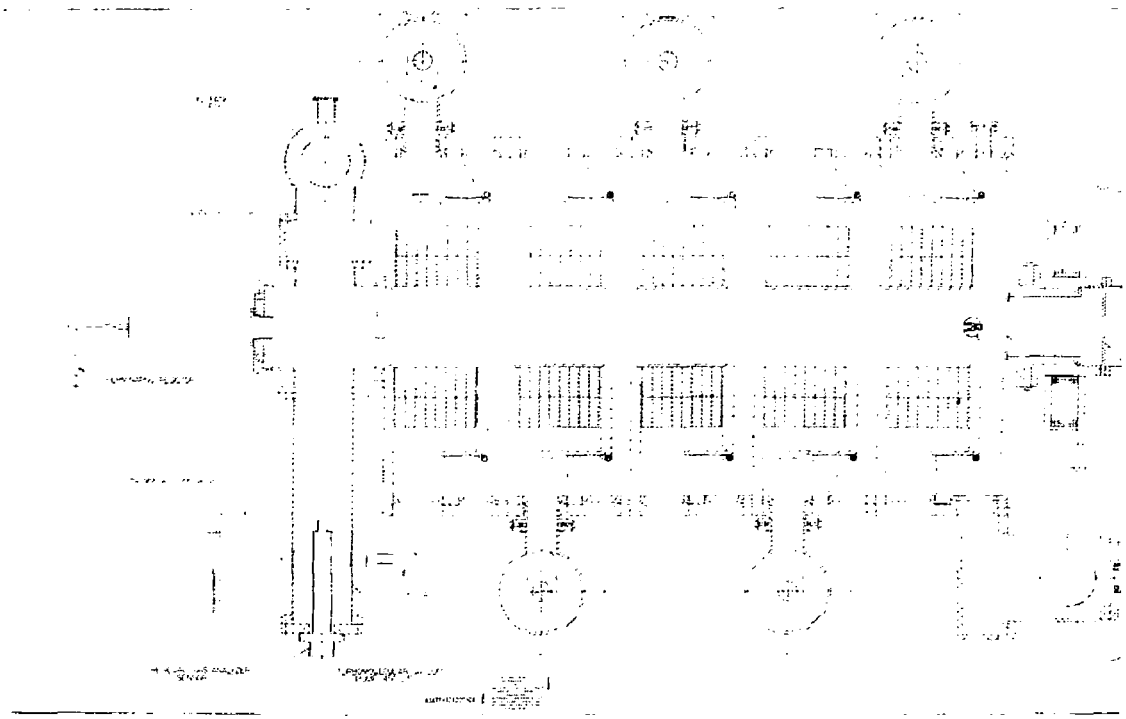

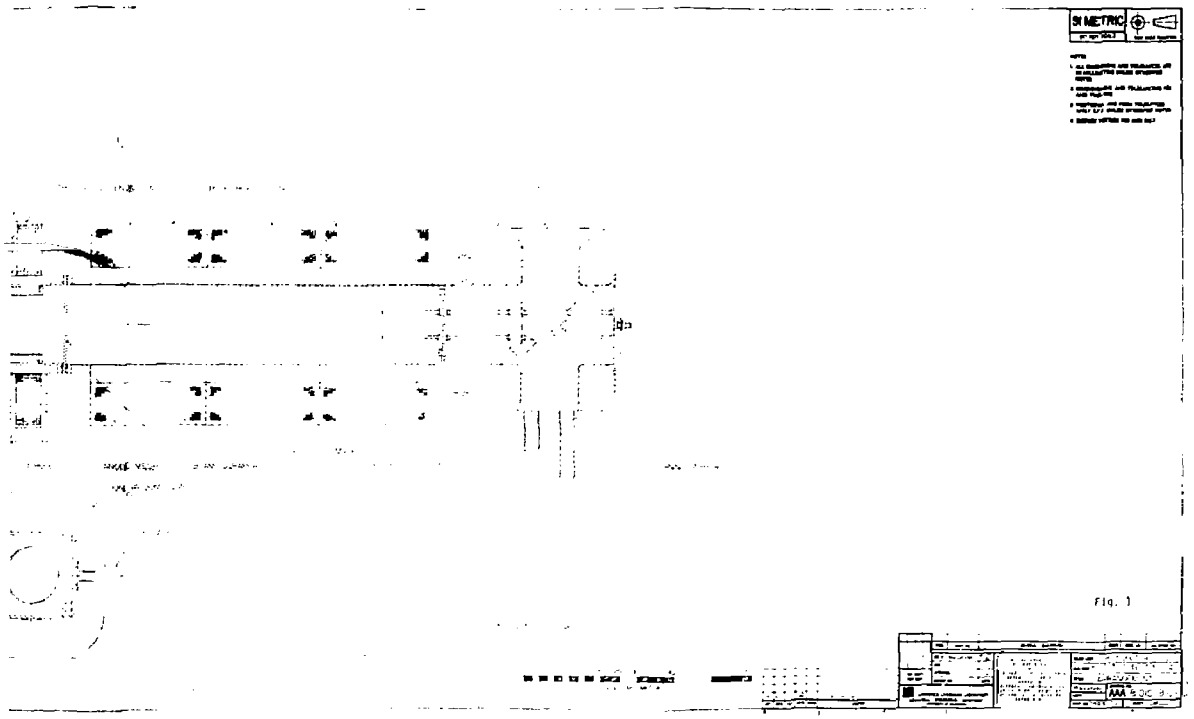

Fig. 1

2

The five accelerating modules each are driven from a 56 ohm Blumlein pulse forming line. Fig. 2 shows an equivalent circuit representation of a typical, single accelerating module. A Marx generator with series capacitance = 3.3 nF and series inductance = 14 μH charges the Blumlein over a period of 400 nsec, after which the Blumlein is discharged into the ferrite filled cavity when the Blumlein switch is fired. The beam current loading of the accelerating gap is represented by a constant current source in parallel with the gap capacitance. A compensating network Z_B is designed to improve the pulse shape of the voltage appearing across the gap.

Typical oscillograms for the charging voltage pulse appearing at each Blumlein center conductor and for the accelerating gap voltage during Blumlein discharge, are shown in Figs. 3 and 4, respectively. The triggering network (Fig. 5) is essentially as described in Ref. 2 with surplus parts omitted.

Beam confinement and focusing beyond the diode is assured by an array of individually controlled solenoids, as shown in Fig. 1. Solenoid S10 was part of the original LBL injector. This solenoid acts as a thin lens with a central field strength of 600-1000 Gauss. The magnetic flux linking the cathode is essentially zero. The "Blue Boy" solenoids, with a typical central field strength of 300-500 Gauss, were used simply to demonstrate beam transmission through the drift space.

Figure 2. Marx/Blumlein/Cavity Circuit Model for Injector Test Stand

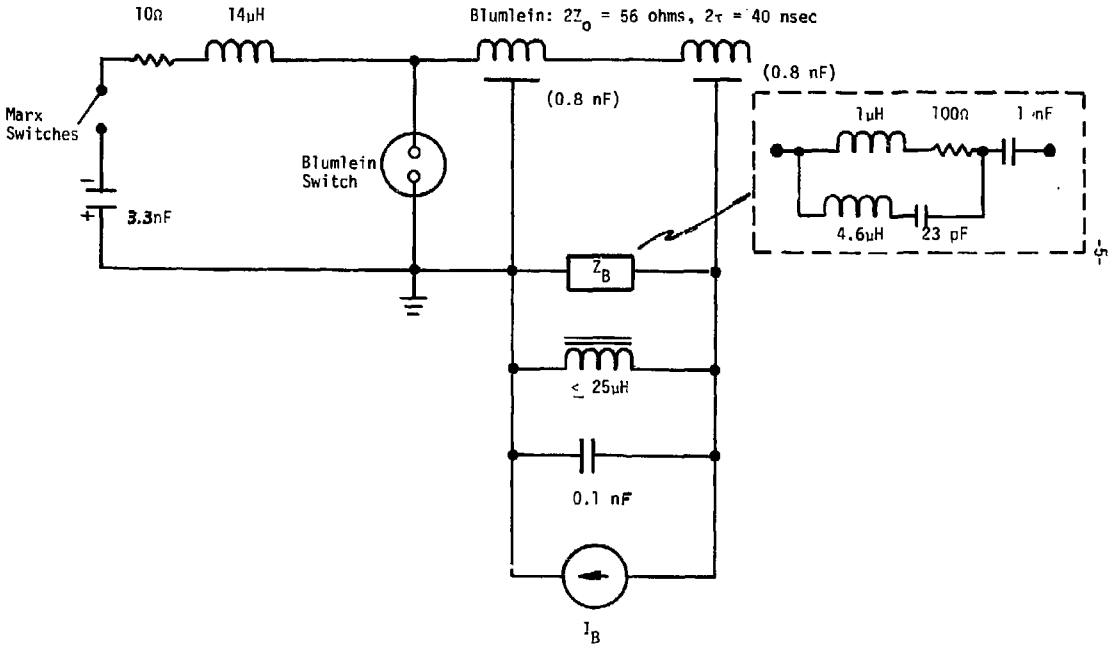

Transmission values of over 80% have been realized with the solenoids set near to their maximum field strength. A typical downstream current waveshape is shown in Fig. 6.

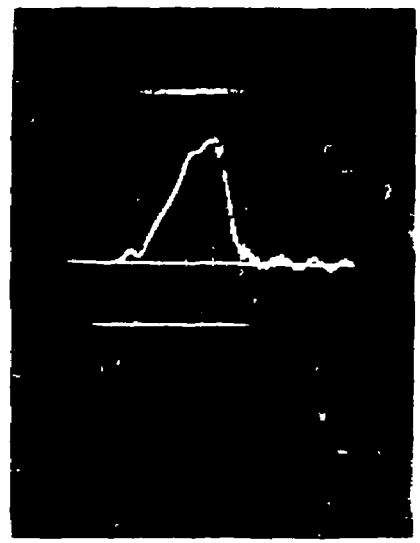

Fig. 3. Typical Blumlein charging waveform. This picture represents 10 successive cycles of Marx generator output, at 50 kV/div and 100 ns/div. The jitter is approximately 20 nsec.

Fig. 4. Typical Blumlein discharge waveform. This picture superimposes 10 successive pulses, at 50 kV/div and 20 nsec/div. The baseline is three divisions from the bottom. The oscilloscope amplifier was set at maximum bandwidth in order to resolve the jitter, here on the order of a few nanoseconds.

Figure 5. Triggering System for Injector Test Stand

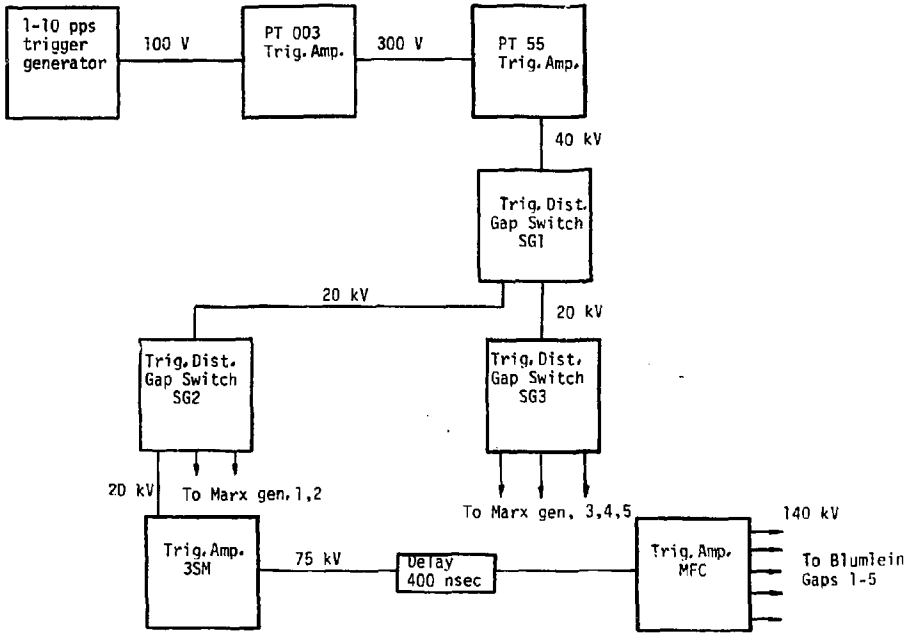

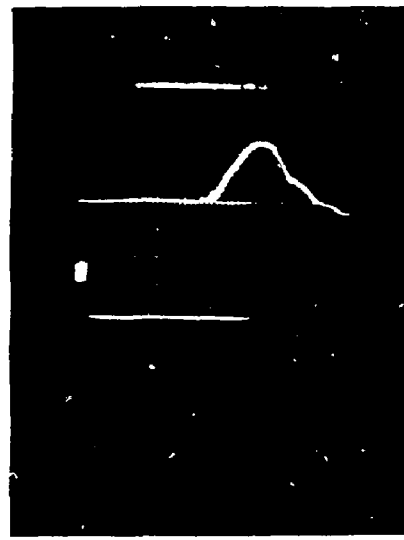

Fig. 6. Typical current waveform. This picture superimposes 25 successive pulses, at 250 A/div, 20 nsec/div. The jitter is approximately 4 nsec RMS.

The one-metre long drift space is terminated by an emittance measuring device consisting of a 1 mm thick, perforated, stainless steel mask ("salt shaker") and a phosphor screen spaced 150 mm downstream. The pinholes in the saltshaker provide a known pattern of beam samples which when photographed at the downstream phosphor target, can be used to estimate the beam emittance. During emittance measurements the last solenoid is turned off so as to minimize the axial magnetic field in the space between the saltshaker and the phosphor target.

The cathode shapes tested here are shown in Fig. 7. These cathodes are threaded directly on to the 13 mm dia cathode stem. Fig. 7a is an LBL design, i.e., an approximately ball shaped, 50 mm dia, stainless steel form with a recessed 9 mm dia emitter button. The latter consists of a seven turn spiral of 25 micrometer Ta tape, resting on its edge. Fig. 7b shows a variation on this design, where the base electrode has been expanded into a pancake shape in order to achieve a more planar anode-cathode configuration.

The 100 mm dia pancake again contains a recessed emitter button (20 mm dia). Fig. 8 shows photomicrographs, with different magnifications, of the 20 mm dia emitter button, after approximately 500 shots. The wear rate appears to be rather small.

(a) Ball-shaped cathode

(b) Pancake cathode

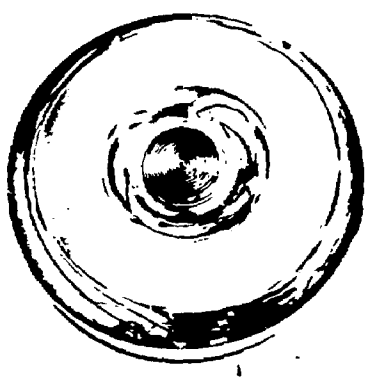

Fig. 7. Cathode Shapes

Fig. 8. Photomicrographs of the 20 mm dia emitter button, after 500 shots.

3. Diode Characteristics

Sophisticated computer codes such as EGUN are available at LLL for guiding the design of space charge limited (Child-Langmuir law) diode electron sources, such as hot cathode guns. The application of a field emitter diode for generating a low-emittance beam is relatively novel, however, and consequently the modeling of such guns is not as well understood. Clearly, it is desirable to qualify the hot-cathode design codes for field emitter design as well. The results to be described in this section indicate field emitter diode behavior that is space charge limited over the range of interest, and thus EGUN and other codes do appear to be applicable.

The field emitter diode consists of the cathode mounted at the end of the cathode stem, facing a mesh anode (0.08 mm tungsten wire on 3.2 mm centers). Using the LBL ball cathode (Fig. 7a), voltage and current measurements were made for different Blumlein voltages and with anode-cathode (A-K) spacings of 10 mm and 40 mm. The voltage appearing across the diode is somewhat less than the sum of the Blumlein voltages because of the potential drop through the Blumlein surge impedance. The ratio of diode current to the 3/2 power of diode potential is plotted in Fig. 9, over the current range 0.5-5 kA. This ratio is called the beam perveance, and its near-constancy (for a given A-K spacing) implies approximately space-charge limited (Child-Langmuir law) operation of this diode.

The observed space-charge limited behavior is consistent with present understanding of field emitter diode operation. True field emission takes place when the diode potential is first applied, from microprotrusions on the cathode surface, here the tantalum spiral. Ohmic heating then causes

the whiskers to melt and evaporate, forming a plasma layer. The latter is polarized by the diode potential, and positive ions maintain sufficient electric field near the cathode for continued electron emission. The electrons, in turn, stream to the anode side of the plasma layer, forming a virtual cathode, i.e., a space-charge limited diode.

Fig. 9 provides further confirmation of Child-Langmuir behavior in that the perveance varies roughly as the inverse square of the A/K spacing.

In conclusion, the similarity in operation to a thermionic diode appears to legitimize the use of standard, thermionic gun design algorithms for optimizing the field emitter diode geometry.

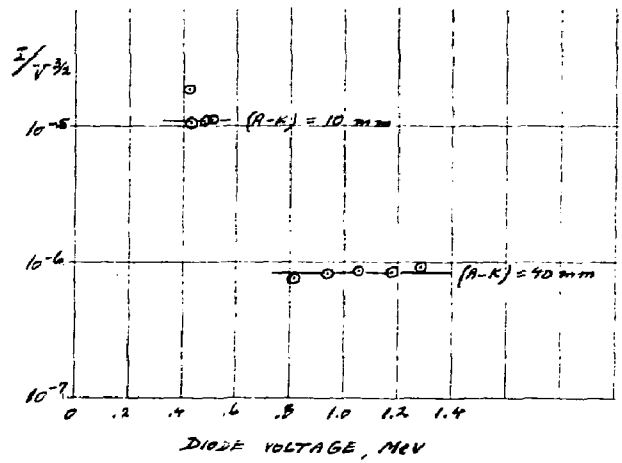

Fig. 9. Perveance of LBL ball diode, for two different A-K spacings. The data points were generated by varying the Blumlein charging voltage from 140-240 kV. The upward shift of one point on the upper curve is thought to be due to random field emission from parts of the cathode ball other than the emitter button. Note the clustering of the high current points due to the potential drop in the surge impedance.

4. Random Field Emission

When the Blumlein generators were charged to 180 kV and beyond, significant variations were observed in the gap voltage amplitude on successive pulses, with modules No. 2 and No. 4. Simultaneously, gas bursts were observed with each pulse. Removal of the cathode stem to eliminate beam loading did not suppress this phenomenon. The random current loading was thus attributed to field emission internal to the modules themselves, probably from the highly stressed outer periphery of the ferrite canister forming part of the negative surface of the accelerating gap. This edge is radiused to 9.5 mm. Further confirmation was obtained on Module 2 by moving an x-ray scintillator plate backed with photographic film around the outer periphery of the module until maximum exposure was found. The emitting area was thus localized in one quadrant of the canister, and it is believed that local surface roughness may be responsible for the emission. In the FXR design for the beam line module, the corresponding corner area has been radiused to 16 mm, and random field emission therefore should be minimal.

5. Dependence of the Gap Voltage on the Ballast Load

The planned increment of accelerator voltage appearing across the gap of each FXR beam line module is nominally 250 kV. However, the modules are being designed to operate without breakdown up to 400 kV, thus allowing the option of increasing the overall beam energy to 24 MeV. The intent is to achieve this voltage enhancement by "matching up," i.e., by delibrately terminating the Blumlein pulse source in an impedance greater than its characteristic (surge) impedance.

This approach was tested on Module 5 of the LBL injector assembly. First, with the ferrite module disconnected, the Blumlein generator was discharged into different purely resistive loads. As shown in Fig. 10, the measured output voltage values agree closely with the prediction from the simple model. Typical waveforms are illustrated in Figs. 11 and 12. The reason for the post-switch ringing on the Blumlein charging waveform, Fig. 11, is not understood, but this in any case does not affect the discharge waveform. The 10-90% risetime on the latter, Fig. 12, is approximately 18 nsec. This is attributed primarily to the switch gap inductance which appears in series with one half of the Blumlein (Z_o = 28 ohms).

Second, the module was reconnected and the Blumlein generator was discharged into the complex impedance load, shown on Fig. 13, consisting of the ballast resistor in shunt with the gap capacitance and the ferrite core inductance. Typical waveshapes are shown in Figs. 14 and 15. The voltage gain here is seen to be much less than would be obtainable with only the ballast resistor, due to the additional loading from the module. In addition, the waveshape has been degraded (no flattop) although this can be compensated, see Fig. 4 above, by using a network of the type shown in Fig. 2. However, the use of the compensating network does not enhance the voltage gain.

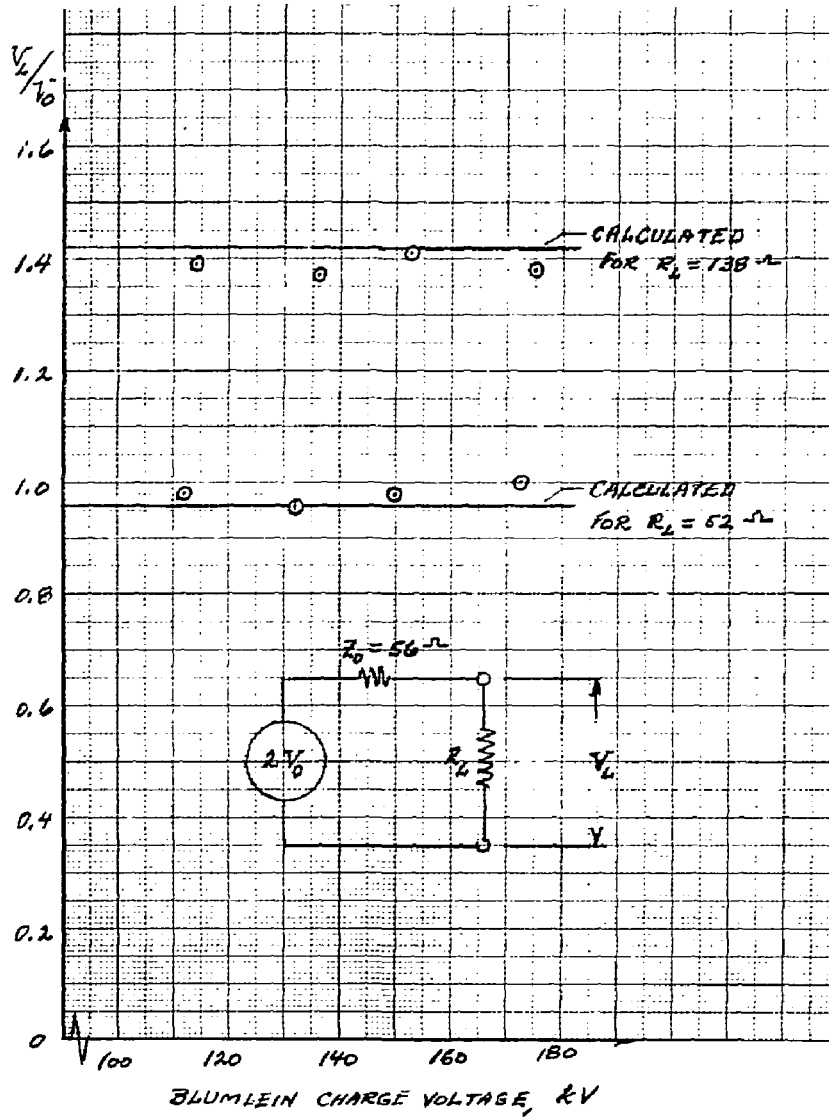

Fig. 10. Measured voltage gain due to Blumlein mismatch into a purely resistive load.

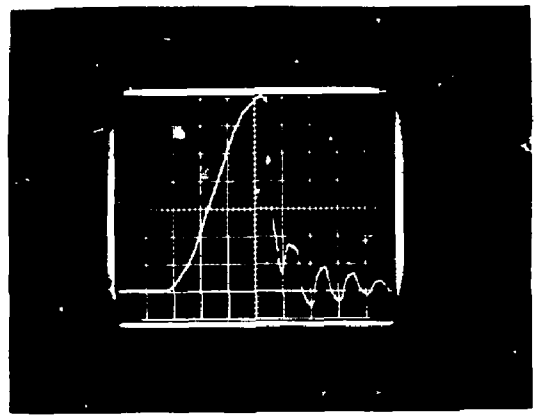

Fig. 11. Typical Blumlein charging waveform with resistive load, R_L = 138 ohms; 25 kV/div and 100 ns/div.

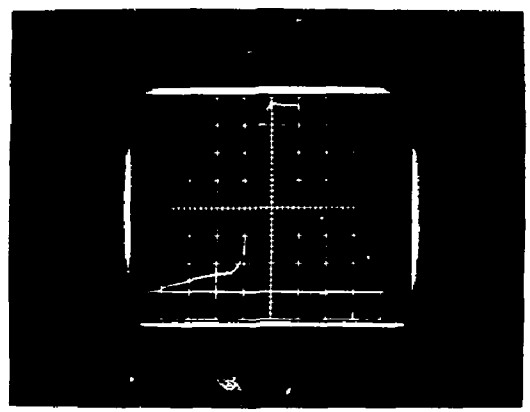

Fig. 12. Typical Blumlein output waveform with resistive load, R_L = 138 ohms; 36 kV/div and 20 ns/div.

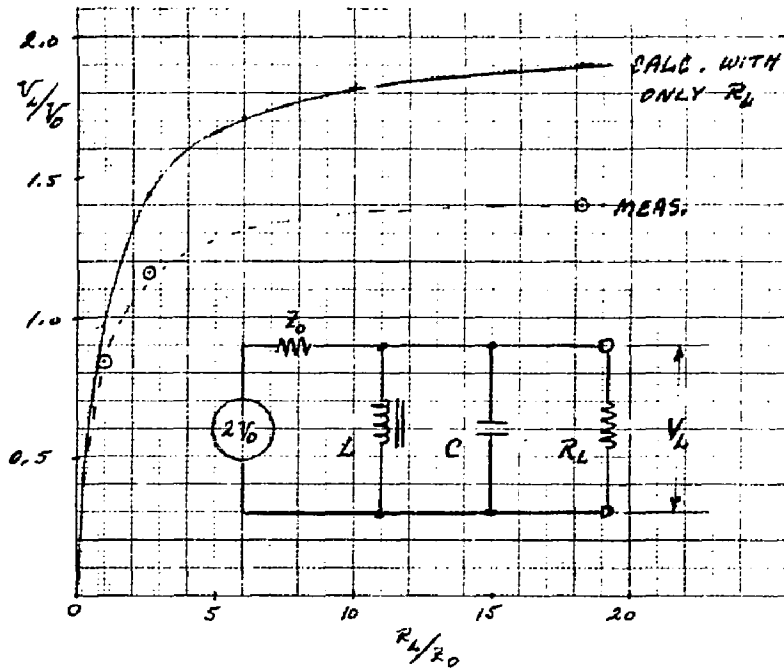

Fig 13. Matched-up voltage ratios for different ballast resistors; No. 5 Blumlein discharging into its accelerating module. The other parameters are Z_0 = 56 ohms, L ≤ 25 μH, C ≈ 100 pF. Each data point represents the average of four measurements, taken at different Blumlein charging voltage levels.

A plausible reason for the poor voltage gain may be found in the gap capacitance, here estimated to be 100 pF. If charged individually through the 56 ohm Blumlein surge impedance, the potential across this capacitance would have a 10-90% risetime of 15 nsec. This is essentially added to the 20 nsec risetime due to the switch inductance, and the output waveform thus never reaches a true peak within the short (40 nsec) duration of the drive pulse. One might also suspect ferrite saturation effects, but

these do not appear to be involved because the FWHM of the output waveshape was observed to be independent of the driving voltage level.

The FXR machine will have both a longer pulse length (90 nsec) and a smaller Blumlein surge impedance (10 ohms), so that the effect of the gap capacitance on the available voltage gain should be much smaller.

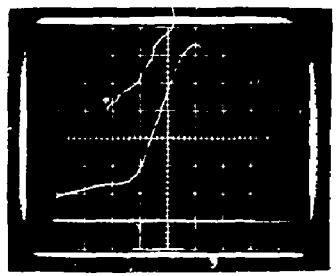

Fig. 14. Blumlein output waveform, discharging into module No. 5, with R_L = 120 ohms; 35 kV/div and 20 nsec/div.

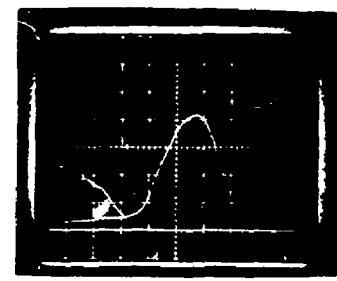

Fig. 15. Blumlein output waveform, discharging into module No. 5, with R_L = 53 ohms; 35 kV/div and 20 nsec/div.

6. Emittance Measurement

The emittance is a figure of merit for the beam quality, and it measures the ease with which a beam can be focused and transported. It is defined as follows (Ref. 3). At each point of any transverse section of the beam, there is an ensemble of rectilinear trajectories that form a cone of angular aperture, 2 $d\alpha$ (Fig. 16). The slope of each ray represents the

ratio of the maximum transverse momentum to the longitudinal momentum for the beamlet emanating from that point. This slope can be plotted as a function of the radius along some transverse direction, assuming a cylindrical beam. As shown in Fig. 16, the beamlet typically undergoes both space charge expansion and transverse displacement so that a range of slope angles $\alpha \pm d\alpha$ is obtained for each transverse position r in the beam.

In this way a phase space diagram of the beam is generated, the area of which is defined as the emittance. The emittance diagram typically approximates the shape of an ellipse.

For a variety of different injection conditions, data obtained with the setup shown in Fig. 1 was used to estimate the emittance. In order to adequately define the beam edge, it was found necessary to collimate the beam at a distance 24 cm from the mesh anode. The upper bound on beam emittance which can be transmitted by the collimator-drift tube combination is called the beam line acceptance, and it is determined simply from the geometry. From Fig. 1, the acceptance is found to be 55 π, 102 π, and 175 π mr-cm for 13 mm, 25 mm, and 50 mm diameter collimators, respectively. Only the 25 mm and the 50 mm collimators resulted in useful images where the beam boundary could clearly be identified on the mask pattern. This already indicated that there was no significant component of beam current with an emittance smaller than that corresponding to the 13 mm aperture, i.e., less than 55 π mr-cm.

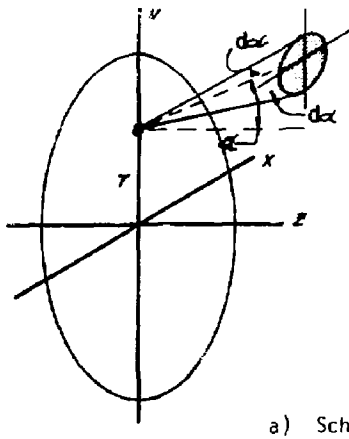

a) Schematic cross section of beam, with elementary beamlet

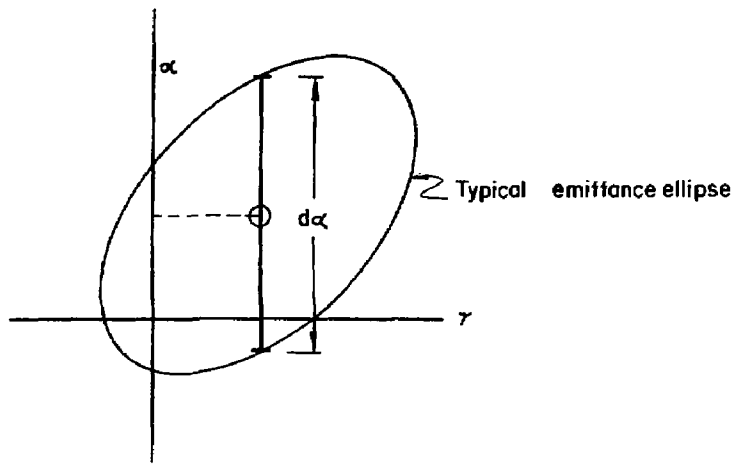

b) Phase plane point corresponding to beamlet in (a)

Fig. 16. Generating a point within the emittance diagram

Emittance diagrams are plotted for both cathodes, for the beam images shown, in Figs. 17 and 18. A line of dots traversing the beam center was chosen for analysis. Each image spot corresponds to a source spot on the hole mask that has undergone both expansion and outward translation.

Allowing for the photographic reduction in size from the real image on the phosphor screen, a Bausch and Lomb measuring magnifier was used to determine each spot size. From the known geometry, the range of angular deflection was then calculated for each beamlet, and this was plotted vs the transverse displacement of the source spot on the upstream hole pattern. For the resulting phase space plots the area of the (approximate) circumscribed ellipse yields the emittance value in each case, as shown. These values are about ten times higher than that desired for the FXR source.

It is difficult to draw a meaningful comparison between the emittance results of Figs. 17 and 18, because the included fractions of emitted beam current are so different. Further emittance measurements are planned where the included fraction is varied systematically, for a single cathode. One does note that the larger-area cathode exhibits a necked-down emittance area, indicating a "cooler" central portion of the beam. i.e., less transverse momentum for electrons near the axis. This might indicate that smaller emitter buttons yield better beams in general. Conversely, it could point to the possibility of generating a lower emittance beam by collimating a high current beam of large cross section down to its cool interior. In

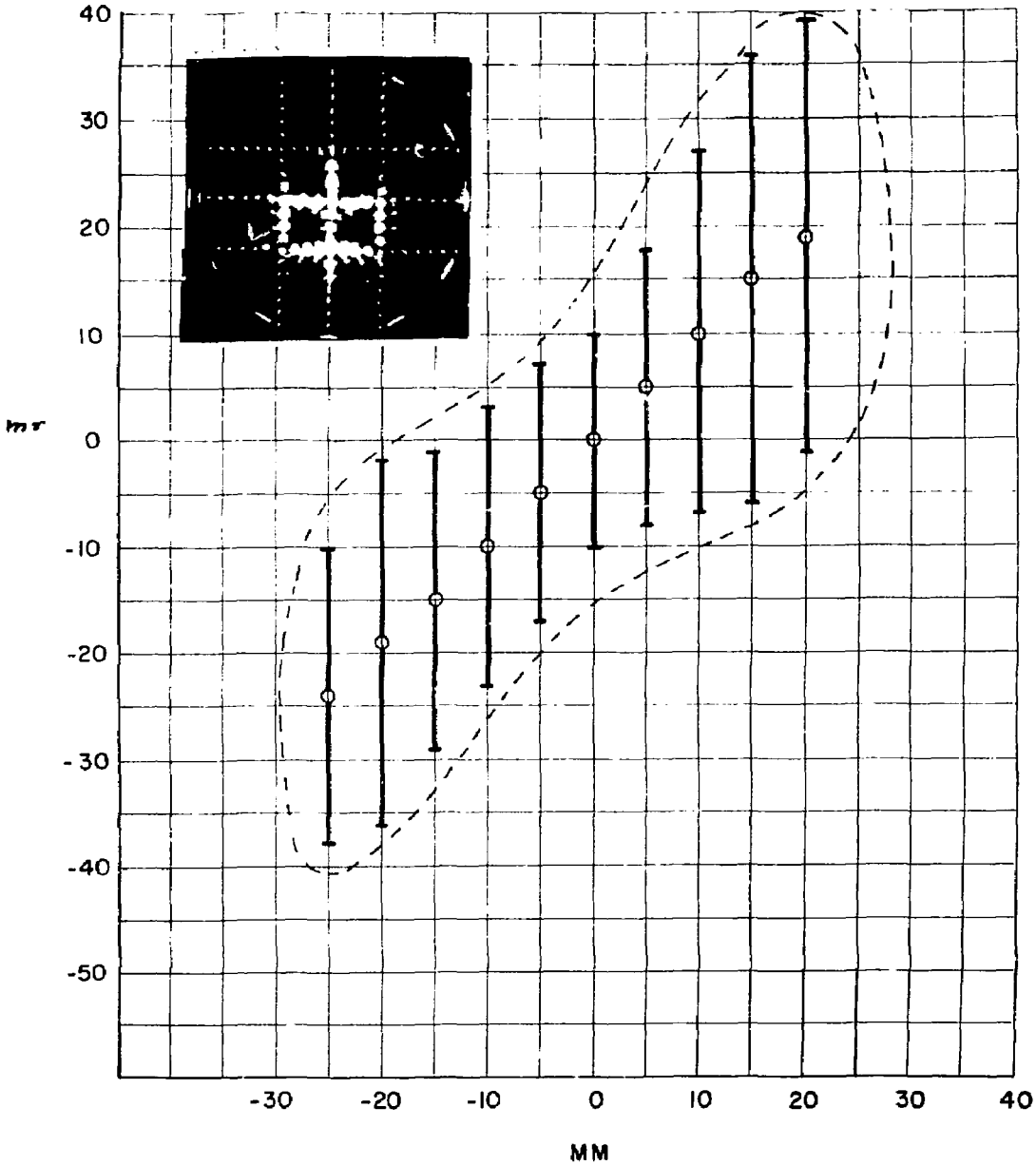

Figure 17. Beam image and phase plane plot, for the pancake cathode with a 20 mm dia emitter. The collimator aperture was 25 mm dia, and the beam parameters are 1.2 MV diode voltage, 1150 A emitted current, 430 A beam current at the emittance target. From this plot, the emittance is estimated at 70 π mr-cm.

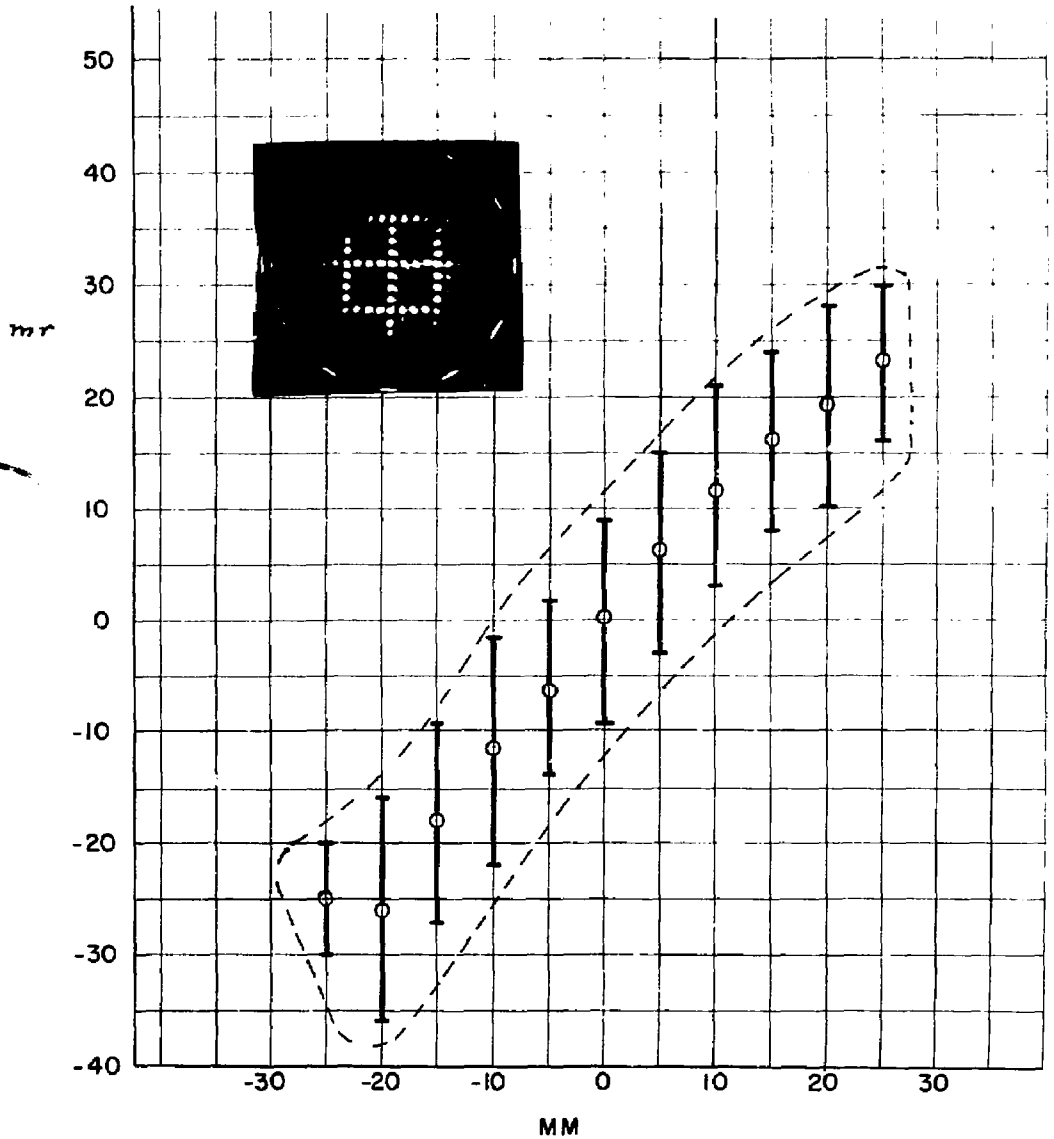

Fig. 18. Beam image and phase plane plot, for the ball-shaped cathode. The collimator aperture was 25 mm dia, and the beam parameters are 1 MV diode voltage, 1980 A emitted current, 285 A beam current, at the emittance target. From this plot, the emittance is estimated at 30 π mr-cm.

any case, careful design effort clearly is required to design a source geometry that will yield the desired cool beam.

7. Conclusion

As part of the current design effort for the FXR machine, the five module injector section of the LBL/ERA linear induction accelerator was brought to LLL and was set up as a test stand. Measurements were carried out to characterize the field emitter diode and the electron beam it generates; to demonstrate simple transport of a high current beam; and to become more familiar with the general circuit properties and operational characteristics of this type of machine.

The field emitter diode was found to be approximately space-charge limited, so that available gun design codes should be applicable for designing the FXR electron source. Beam transport with axial confining fields of less than one kilogauss appears to be straightforward. However, the measured beam emittance turned out to be much higher than that desired for the FXR machine, and careful effort will be required to design a source geometry that will produce the desired cool beam.

References

1. High Explosive Flash Radiography Facility, System Design Requirements, Project No. 78-16-C, Lawrence Livermore Laboratory, January, 1978.

2. R. Avery, et. al., The ERA 4-MeV Injector, Trans. IEEE NS-18, pp. 479-483 (1971).

3. A. Septier, Focusing of Charged Particles, VII, p. 150, Academic Press, N.Y., (1967).